Early increase in apparent diffusion coefficient predicts favorable response to Dordaviprone (ONC201) therapy in H3K27M-mutant diffuse midline glioma

Benison C Lau, Diala P Ajaero, Benjamin A Hoff, Ashley Pearson, Peter Sajjakulnukit, Jack Wadden, Tiffany Adam, Sunjong Ji, Adam L Green, Ali Nabavizadeh, Yue Cao, Madhava Aryal, Santhosh Upadhyaya, Andrea Franson, Stefanie Galban, Sriram Venneti, Bryan Federowicz, Mark A Shapiro, Timothy J Stuhlmiller, Costas Lyssiotis, Craig J Galban, Hemant A Parmar, Mohannad Ibrahim, Carl Koschmann

Early increase in apparent diffusion coefficient predicts favorable response to Dordaviprone (ONC201) therapy in H3K27M-mutant diffuse midline glioma

Authors:
Benison C Lau[1,2], Diala P. Ajaero[1], Benjamin A. Hoff[3], Ashley Pearson[1], Peter Sajjakulnukit[4], Jack Wadden[1], Tiffany Adam[1], Sunjong Ji[1], Adam L Green[5], Ali Nabavizadeh [6], Yue Cao[7], Madhava Aryal[7], Santhosh Upadhyaya[1], Andrea Franson[1], Stefanie Galban[3], Sriram Venneti[8], Bryan Federowicz[9], Mark A. Shapiro[9], Timothy J. Stuhlmiller[9], Costas Lyssiotis[4], Craig J. Galban[3], Hemant A. Parmar[3], Mohannad Ibrahim[3], Carl Koschmann[1]*.

Affiliations:
[1]Department of Pediatrics, University of Michigan Medical School, Ann Arbor, MI, USAi
[2]Pediatric Neuro-Oncology Program, UPMC, Pittsburgh, PA, USA
[3]Department of Radiology, University of Michigan Medical School, Ann Arbor, MI, USA
[4]Department of Molecular and Integrative Physiology, University of Michigan, Ann Arbor, MI, USA
[5]Morgan Adams Foundation Pediatric Brain Tumor Research Program, Department of Pediatrics, University of Colorado Anschutz School of Medicine, Children's Hospital Colorado, Aurora, CO, USA
[6]Department of Radiology, University of Pennsylvania Perelman School of Medicine, Philadelphia, PA, USA.
[7]Department of Radiation Oncology, University of Michigan, Ann Arbor, MI, USA
[8]Department of Pathology, University of Michigan Medical School, Ann Arbor, MI, USA
[9]xCures, Inc., Oakland, CA, USA

Running title:
Diffusion and ONC201 response in H3K27M-DMG

***Correspondence:**
Carl Koschmann
University of Michigan Medical School
3520D MSRB I, 1150 W Medical Center Drive
Ann Arbor MI, 48109
Phone: 734-936-9814
Fax: 734-763-2543
Email: ckoschma@med.umich.edu

Conflict of interest:

Authorship:
All authors have contributed in meaningful ways and reviewed the manuscript.

Total manuscript word count (abstract, text, references, and figure legends): 6527

Abstract (250 words):

Background:

Dordaviprone (ONC201) is the first FDA-approved therapy for H3K27M-mutant diffuse midline glioma (DMG). However, therapeutic response varies among patients, and no imaging biomarkers currently predict long-term benefit. Diffusion-weighted MRI and apparent diffusion coefficient (ADC) obtained during standard clinical imaging reflects tissue cellularity and necrosis, offering potential as an early response indicator.

Methods:

Clinical and imaging data from patients treated with dordaviprone (n=83) on completed studies underwent centralized neuroradiology review, ADC histogram analysis, and Functional Diffusion Mapping (fDM), which were compared and correlated to CSF tumor DNA (tDNA) and metabolomics when available. Final analysis included 38 patients receiving standardized dordaviprone dosing and treatment schedule.

Results:

In the pre-progression cohort, early changes in volumetric or cross-sectional RAPNO criteria were not predictive of overall (OS) or progression-free survival (PFS). Importantly, in patients treated pre-progression with dordaviprone post-radiation, tumors with increased diffusion ADC (reduced cellularity) at cycle 3 demonstrated median OS of 732 days versus 360 days for those with decreased ADC (increased cellularity, $p = 0.0149$); with corresponding PFS of 334 versus 110 days ($p = 0.0132$).

fDM analysis of spatio-temporal changes of ADC did not correlate with outcomes in a sub-cohort analysis but demonstrated predictive patterns in individual patient time course series. CSF metabolomics stratified by ADC change revealed differences in reductive stress metabolites among dordaviprone responders, linking ADC elevation to dordaviprone -driven metabolic effects.

Conclusion:

Early increase in ADC correlates with improved response to dordaviprone in H3K27M-DMG and correlates with CSF metabolic changes, suggesting ADC warrants prospective validation as a biomarker.

Keywords:

Diffusion-weighted imaging, Apparent Diffusion Coefficient, Diffuse Midline Glioma, Diffuse intrinsic Pontine Glioma, Brain tumor

Key Points (260 characters):

- Early ADC measurements may correlate with long term response to dordaviprone
- Changes in histogram ADC assessment better correlate with long term response than size-based assessments
- ADC response correlates with CSF metabolites shifts expected with dordaviprone therapy

Importance of the Study (150 words):

Dordaviprone (ONC201)is the first FDA-approved therapy for H3K27M-mutant diffuse midline glioma (DMG). We present the first advanced radiological biomarker associated with long-term dordaviprone treatment response in patients with H3K27M-mutant DMG and diffuse intrinsic pontine glioma (DIPG). Among patients receiving dordaviprone as upfront therapy after radiation, an early increase in apparent diffusion coefficient (ADC) values after two treatment cycles correlated with improved clinical outcomes, identifying an early and measurable potential radiographic biomarker of therapeutic response. Because diffusion MRI is routinely performed alongside standard MRI in clinical practice, these findings provide a readily accessible imaging marker that may provide monitoring treatment benefit. Prospective validation in independent cohorts is needed before clinical implementation. This study suggests diffusion-based MRI as a valuable tool in the management of H3K27M-DMG and DIPG and advances understanding of how diffusion imaging can inform care and prognosis across pediatric and adult brain tumor populations.

Introduction

Diffuse midline gliomas (DMG) harboring H3K27M alterations are associated with aggressive clinical behavior with median overall survival (OS) of 11 to 15 months.[1,2] DMG and diffuse intrinsic pontine gliomas (DIPG) arise in midline central nervous system (CNS) structures, primarily the thalamus and brainstem,[1] where surgical resection and biopsy assessments are limited and no curative systemic therapy has been identified.[2,3]

Magnetic resonance imaging (MRI) remains the primary tool for diagnosis, disease monitoring and treatment guidance of DMG.[4,5] Response assessments primarily rely on changes in cross-sectional area, development of new lesions, or clinical deterioration. While volumetric assessment may improve accuracy in identifying progressive disease and more reliably predict clinical outcomes, size-based measurement remain difficult due to poor inter-operator reliability,[6] and are limited in their ability to predict overall outcomes.[7] Diffusion weighted imaging (DWI) is acquired during clinical imaging, providing adjunctive information reflecting cellularity and inflammation, and potentially additional insight into response in these tumors. DWI has identified baseline characteristics predictive of overall outcome[8,9], demonstrated utility in clarifying pseudo-progression[10]. However, histogram analyses and spatio-temporal analysis using functional diffusion mapping (FDM) have not identified clear changes that correspond to outcomes[8,9].

Dordaviprone (ONC201), a ClpP agonist and dopamine receptor D2 (DRD2) antagonist, received accelerated FDA approval in 2025 for the treatment of patients with progressive H3K27M DMG. In a retrospective analysis of data from 4 clinical trials and 1 expanded access protocol ONC006 NCT02525692, ONC013 NCT03295396, ONC014 NCT03416530, ONC018 NCT03134131, and ONC016 NCT05392374, 50 post progression patients treated with dordaviprone revealed overall response rate of 20% with median duration of response 11.2 months.[11] dordaviprone exerts its anti-tumoral activity by inactivation of AKT and ERK through the integrated stress response[12,13] and activation of mitochondrial caseinolytic protease P (CLPP).[14]

In an exploratory retrospective review of combined data from ONC014 (NCT03416530) and ONC018 (NCT03134131), we found OS and progression free survival (PFS) of 21.7 months and 7.3 months, respectively, in patients treated after radiation but prior to progression (non-recurrent), which compared favorably to historical control data.[15] Further, when assessing tricarboxylic acid cycle (TCA)–related genes, dordaviprone treatment increased 2-

hydroxyglutarate (2-HG) in H3K27M-DMG cells and patient cerebrospinal fluid (CSF), leading to restoration of repressive H3K27me3 and downregulation of genes controlling the cell cycle and neuroglial differentiation. Overall, these results support that H3K27M-DMG cells has unique sensitivity to dordaviprone disrupting interconnected metabolic and epigenetic pathways and reversing hallmark H3K27me3 loss.[15]

Despite this promise, many patients with H3K27M DMG have no response to dordaviprone and to date there are no predictors of which patients might have benefit. Further, no imaging modalities during treatment have proven successful at predicting outcomes in H3K27M-DMG. This may be in part due to the homogeneously poor outcomes that have been seen with historical therapeutic trials. The small portion of longer-term survivors of early phase dordaviprone [11] or recent CAR-T trials[16,17] may open the door to predictive biomarkers to capture the heterogeneity of response. Indeed, we previously showed that early changes in serial CSF and plasma H3K27M cell-free tumor DNA (cf-tDNA) correlate with long-term outcomes of dordaviprone treatment.[18] To our knowledge, the feasibility and utility of diffusion-weighted imaging techniques monitoring response to this promising therapy has not been established.

Here, we report a retrospective analysis of imaging characteristics from patients treated with dordaviprone therapy for H3K27M-DMG and DIPG, comparing clinical outcomes to anatomic assessments, diffusion imaging parameters, and fDM analysis. Diffusion characteristics were compared to CSF tumoral DNA and CSF metabolomics at similar timepoints. The results of our analysis demonstrate that early changes in diffusion imaging may correlate with long-term response in patients with non-recurrent H3K27M-DMG and demonstrate metabolic changes correlating to dordaviprone mechanism of action.

Materials and Methods

Subjects:

Our analysis included patients treated in two studies: (i) a multisite clinical trial in children and adolescents with H3K27M-mutant DMG (NCT03416530, ONC014) and (ii) a multisite expanded access protocol study in children and adults with H3K27M-mutant DMG (NCT03134131, ONC018). This was a retrospective study approved by the institutional review board (HUM00267324, HUM00247755 and HUM00245122) and performed in accordance with the Declaration of Helsinki. Patients who were clinically diagnosed with DIPG or non-spinal biopsy-

proven H3K27M DMG seen at C.S. Mott Children's Hospital or University of Michigan between 2018 and 2024 were reviewed.

Additional patients were identified from the XCELSIOR Database (NCT03793;088), a non-interventional data registry through which patients were enrolled on their own behalf or by their legally authorized representatives via electronic consent. Patients signed a HIPAA release to permit aggregation of deidentified electronic medical records and data structuring from all sites of care. This retrospective use was considered not regulated by University of Michigan IRB (HUM00247755), a data use agreement was completed.

To be included in final analysis, patients must have been diagnosed with H3K27M DMG, identified on biopsy or radiographic DIPG, and received monotherapy treatment with dordaviprone at phase 2 weight-based once weekly dosing (625 mg for patients ≥18 years of age, or a dose based on body weight for patients <18 years of age). Patients must have diffusion imaging, including apparent diffusion coefficient at set timepoints (baseline, post radiation and/or cycle 3 of dordaviprone). Patients in the pre-progression post-radiation cohort started dordaviprone 4-14 weeks from the end of radiation. Post-progression patients started dordaviprone concurrently or after re-irradiation.

Exclusion criteria include any patient with spinal primary DMG, participation in placebo-controlled trials, unmeasurable disease at cycle 3, patients with confirmed non-traditional dosing of dordaviprone, patients with non-traditional timing of ONC201 initiation, or H3 wildtype.

Overall survival was measured for all patients, calculated as the length of time from radiographic diagnosis to death and/or the last follow-up. In the post-progression cohort, survival was calculated from the most recent date of progression before starting dordaviprone. Progression free survival (PFS) was measured using Response Assessment in Pediatric Neuro-Oncology (RAPNO) criteria.[4,5] Chart review was utilized for clinical deterioration and size criteria was derived from centralized review by two expert neuroradiologists.

Treatment course and Imaging timepoints

Patients were separated into homogenous treatment groups based on treatment initiation prior to (pre-progression) and post-progression cohorts. The pre-progression cohort was further divided into patients receiving dordaviprone co-current with upfront radiation (54-60 gray) and patients receiving dordaviprone only post-radiation, defined as initiation of dordaviprone 4-14 weeks from end of radiation.

In the pre-progression cohort, baseline was considered the timepoint prior to upfront radiation and dordaviprone. Patients receiving dordaviprone co-current with radiation post-radiation timepoint represented the first imaging timepoint following initiation of dordaviprone. For patients receiving pre-progression with dordaviprone initiated post-radiation, post-radiation timepoint occurs after completion of radiation prior to initiation of dordaviprone, and cycle 3 represents the first imaging timepoint following initiation of dordaviprone.

In the post-progression cohort, patients were treated following first or second progression. Baseline was considered imaging timepoint prior to initiation of dordaviprone or re-irradiation, with cycle 3 occurring 2 cycles following initiation of dordaviprone.

Imaging Analysis

Two senior neuroradiologists (HP twenty years' experience and MI twenty-one years' experience) performed centralized review. Each case was reviewed by one of the neuroradiologists and measurements were completed in accordance with RAPNO recommendations[4,5]. Imaging was collected in both 1.5T and 3.0T scanners. When available 3D imaging was preferentially used for imaging analysis. DWI imaging was completed at b-values of 0 and 1000. Cross-sectional area was determined using T2 FLAIR or T2 weighted imaging. Using the axial image featuring maximal tumor area, the tumor area was calculated as the product of this maximal diameter measurement and the diameter, perpendicular in the same plane.

Volumetric analysis of the tumor was obtained by manually segmentation for 3D volumes of interest (VOIs) on ITK-SNAP (www.itksnap.org).[19] This procedure was performed on the T2 weighted imaging primarily T2-FLAIR imaging by delineating the abnormal T2-hyperintense signal. When T2 FLAIR was unavailable, this parameter was estimated using T2-weighted sequences. To generate the ADC histogram, we completed a rigid co-registration of the ADC maps to the anatomic sequence of interest (T2 FLAIR or T2) using an in-house functional image analysis tool (imFIAT).[20] Within each tumor, values of the mean, SD, median, skewness, and kurtosis of the ADC histogram for the total tumor volume and largest single slice were used for statistical analysis. ADC histogram was normalized to exclude values less than 600 or more than 2600 to automatically exclude cysts, necrosis, and hemorrhage.[9,10] VOIs were manually reviewed after co-registration to exclude areas where registration errors had occurred.

Functional Diffusion Mapping

Anatomical images and ADC maps were co-registered to the pretreatment MRI using a deformable image registration algorithm optimized with mutual information (Elastix).[21,22] Briefly, ADC maps were first aligned to their corresponding anatomical images at each time point. Subsequently, post-therapy anatomical images were aligned to pre-therapy images, and the resulting transformation matrices were then applied to the post-therapy ADC to match the geometric frame of the pre-therapy anatomical images. Tumor regions of interest (ROIs) were delineated on T2-weighted images, primarily FLAIR, at both time points. Eligibility requires a minimum of 4 mL of tumor on postoperative scans. For fDM analysis, only voxels common to both the pre- and post-therapy tumor volumes were considered. Individual voxels were classified into three categories based on the change in ADC from the pretreatment scan to each time point. Red voxels represented areas within the tumor where ADC increased ($> 55 \times 10^{-5}$ mm^2/sec), blue voxels represented decreased ADC ($< 55 \times 10^{-5}$ mm^2/sec), and green voxels represented no change. This threshold represent the 95% CI for change in ADC for uninvolved cerebral hemisphere.[23] The proportion of tumor within these categories was calculated as fIADC (increase), fDADC (decrease), and fnADC (no change).

CSF Analysis

CSF analysis were previously performed on a subgroup within this cohort. Patients in a phase 1 trial for dordaviprone in the pre-progression and post-progression setting underwent CSF collection at baseline, 2, and 6 months from treatment. CSF H3.3 tumoral DNA was assessed using the Bio-Rad QX200 AutoDG system, with analysis completed using QuantaSoft Analysis Pro (Bio-Rad) while multi-gene molecular assessment was previously completed using ultra-short fragment (100-200bp) PCR amplification of cf-tDNA with rapid amplicon-based sequencing by Oxford Nanospore Technology quantification of VAF.

For CSF metabolomics, liquid chromatography coupled with tandem mass spectrometry (LC/MS-MS) was conducted following previously established procedures[24]. Specifically, we employed an Agilent 1290 UHPLC system coupled with a 6490 Triple Quadrupole (QqQ) Mass Spectrometer for label-free targeted metabolomics analysis. A negative ion mode was utilized to acquire coverage of 240 metabolites including metabolites involved in glycolysis, TCA, PPPP, nucleotides, and amino acids.

Statistical Analysis

Clinical and demographic variables were summarized using descriptive statistics. Continuous measures were summarized using medians and ranges. Categoric measures were summarized using frequencies and proportions. Continuous variables (mean ADC, median ADC) were dichotomized on the median value at various timepoints (baseline, post radiation and cycle 3) and tested for association with OS or PFS using Mann-Whitney testing. Continuous variables (mean ADC, median ADC) were further stratified by the difference between baseline to post radiation, baseline to cycle 3, and post radiation to cycle 3 and tested for association with OS or PFS utilizing Spearman's correlations. Differences in OS and PFS were determined via Kaplan-Meier analysis and cox proportional hazards. Change in ADC analysis was completed, based on the difference of mean ADC values between two timepoints. Data were considered significant if *p* values were below 0.05. Metabolomic analysis was performed using multiple *t*-tests to generate a volcano plot, and multiple-hypothesis testing was controlled using a two-stage step-up procedure with a 1% false discovery rate. GraphPad Prism (version 10.4.1) R (version 4.5.2), and Microsoft Excel (Version 2025) were utilized for statistical analyses and figure generation.

Results

Baseline Patient characteristics.

A total of 83 patients with DIPG or DMG were screened for inclusion in analysis. 50 patients were excluded due to inadequate imaging (24), not receiving dordaviprone or receiving incorrect dose (9), presence of a spinal primary tumor (6) or trials that use dordaviprone in combination with another therapy (3) or due to blinded and placebo-controlled trial design (2) (Figure 1B). Additional patients were excluded, such as long-term survivors with no measurable disease at cycle 3 (3), patients with atypical timing of initiation of dordaviprone (3), or where treatment began greater than 14 weeks from radiation (3).

Twenty-seven pre-progression and eleven post-progression patients underwent analysis. The pre-progression cohort included 18/27 pontine, 8/27 thalamic, and 1/27 cortical primary tumors (Figure 1C). The pre-progression co-current radiation cohort had median OS of 309.5 days, median PFS of 150 days. The pre-progression post-radiation cohort median OS was 481.5 days and PFS 140 days. Biopsy was completed in 23/27 patients with additional sequencing completed in 18/23 patients (Figure 1D-E). The most prevalent mutation within this cohort was

H3.3 alterations (14/18), whereas two individuals had H3.1 alterations. TP53 and ATRX mutations were also prevalent, comprising 10/18 and 4/18 of the pre-progression cohort, respectively (Figure 1F).

Within the pre-progression post-progression cohort, mean age was 13 years old (range 3-44), primary location of DMG was brainstem in 14 patients, thalamic in six patients, and one patient had cortical disease. Diagnosis was confirmed with pathology review in 18 patients. (Table 1)

Size based characterization of patients on dordaviprone does not predict overall response.

To determine whether early changes in conventional imaging response metrics were associated with clinical outcome, we first evaluated dordaviprone -treated patients using standard two-dimensional measurements in accordance with RAPNO for DIPG[4] for pontine lesions and RAPNO for high grade glioma[5] for non-pontine H3K27M DMG and volumetric assessments (n=21). Centralized radiographic review according to RAPNO criteria revealed that, within the pre-progression post-radiation cohort initiating dordaviprone (n=21), there was significant variability in response: seven patients achieved a minor or partial response, three had progressive disease, and the remaining patients demonstrated stable disease (Figure 2A-B).

Using cross-sectional area by RAPNO criteria, we compared patients with increasing and decreasing size from baseline to cycle 3 according to RAPNO criteria, there was no significant difference in OS (Cox PH p = 0.2274, Figure 2C) or PFS (Cox PH p = 0.22, Figure 2G). These findings were consistent findings with our observations of volumetric (3D) measurements, which similarly demonstrated no association with OS (Cox PH p = 0.469, Figure 2D) or PFS (Cox PH p = 0.384, Figure 2H). Spearman correlation analyses further confirmed the absence of a significant relationship between change in cross-sectional area and OS (r = 0.1865, p = 0.43, Figure 2E) or PFS (r = –0.2266, p = 0.3956, Figure 2I). Likewise, changes in tumor volume between baseline and cycle 3 were not correlated with OS (r = 0.24, p = 0.30, Figure 2E) or PFS (r = 0.30, p = 0.25, Figure 2I). Cross-sectional and volumetric measurements were highly concordant across timepoints, with a strong correlation between percentage change in cross-sectional area and volume (r = 0.93, p= 0.00000517, Supplementary Figure 2C).

MRI diffusion analysis of pre-progression, post-radiation dordaviprone patients

Patients in the pre-progression, post-radiation dordaviprone initiation cohort (n=21) received standard-of-care radiotherapy (54–60 Gy) followed by initiation of dordaviprone therapy 4–14 weeks after radiation completion (Figure 3A). When stratified by median ADC(10^{-3} mm²/s) values at baseline, post-radiation, and cycle 3, there were no significant differences in OS or PFS (Supplementary Figure 3A-B). Likewise, ADC values at individual timepoints were not correlated with OS or PFS (Supplementary Figure 3C-D), indicating that single timepoint diffusion measures were not predictive of outcome.

To explore the predictive value of diffusion imaging, patients were stratified based on whether total tumor volume experienced an increase or decrease in mean ADC from baseline to cycle 3 (median 174 days, range 120-220 days) (Figure 3B). Individuals with increased ADC trended towards longer survival (Figure 3C). Cox proportional hazards analysis revealed that patients with decreased ADC had significantly shorter median OS (360 days) and PFS (110 days) compared to those with increased ADC (median OS 732 days; PFS 334 days). For OS, the hazard ratio was 0.695 (95% CI 0.519-0.93, p=0.0149) per 0.1x 10^{-3} mm²/s increase in ADC sand in PFS hazard ratio per 0.1x 10^{-3} mm²/s increase was 0.027 (95% CI 0.002-0.472, p=0.0132) (Figures 3D–3E). Change in ADC was positively correlated with both overall survival ($r = 0.54$, $p = 0.0119$) and progression-free survival ($r = 0.56$, $p = 0.0132$) (Figures 3F), indicating that increases in ADC from baseline to cycle 3 are associated with improved clinical outcomes and may serve as an early imaging marker of therapeutic response.

When further stratified by tumor location, among patients with brainstem gliomas (DIPG) (n=14), those with decreased ADC had a median OS of 353.0 days compared to 616.0 days in patients with increased ADC (Figure 3I). Although OS was significantly longer in the increased ADC group, PFS did not differ significantly median (110 vs. 183.5 days). (Figure 3I-J).

Similar analyses comparing ADC changes between baseline and post-radiation (n=17) (occurring median 33 days, range 2-84 days from end of radiation), and between post-radiation and cycle 3 (n=18), did not identify statistically significant associations with OS or PFS (Supplementary Figure 3E-H). Exploratory analyses of additional ADC histogram features, including median , kurtosis, and skewness, showed no association between baseline, post-radiation, or cycle 3 characteristics and clinical outcomes. Further changes in median ADC between timepoints did not correlate with OS or PFS. (Supplementary Figure 4).

MRI diffusion analysis of (1) pre-progression patients treated concurrently with dordaviprone and initial radiation and (2) patients treated at recurrence

In the pre-progression cohort treated with concurrent dordaviprone and radiation (n = 6), ADC assessments were completed from baseline to post-radiation timepoint (Supplementary Figure 5A). Analysis was limited by small sample size and minimal response variability (median OS 309.5 days; PFS 150 days) (Supplementary Figure 5B-C). Stratification by median ADC at baseline, or end of radiation, showed no significant differences in OS or PFS, and ADC values were not correlated with survival outcomes (Supplementary Figure 5E-G). Longitudinally, seven of eight evaluable patients demonstrated decreasing ADC from baseline to post radiation limiting stratification by direction of change (Supplementary Figure 5C).

In the post-progression cohort (n = 11), patients received dordaviprone after a mean of 1.1 prior therapies and a median of 441 days from diagnosis (Supplementary Figure 6A-B). Best responses included partial response in 4 patients, stable disease in 4, and progression in 3. (Supplementary Figure 6C-D)

In the post progression population, stratification by cross-sectional area per RAPNO criteria and volumetric analysis showed no significant differences in OS or PFS (Supplementary Figure 6E-F). Mean ADC at progression and cycle 3, as well as changes in ADC between progression and cycle 3, were not associated with differences in OS or PFS (Supplementary Figure 6G-N).

fDM and integrated CSF analysis

Given the spatial heterogeneity of DMG, we next applied fDM analysis to capture spatio–temporal changes in ADC. This analysis, performed in a subset of pre-progression, post-radiation patients (n = 11), quantified the fraction of voxels with increased (fIADC) or decreased (fDADC) ADC and their ratio (FDM ratio, fIADC: fDADC). None of these paramete33rs, analyzed between baseline and cycle 3, correlated with OS or PFS, and stratification by FDM ratio (≥1 vs. <1) similarly revealed no significant survival differences by log-rank analysis (Supplementary Figure 7).

To explore whether diffusion-based imaging changes reflected underlying molecular tumor dynamics, we integrated fDM with previously obtained serial CSF cell-free tumor DNA (tDNA) data[18,25] in an exploratory cohort of pre-progression patients (n=4). Within the limits of the samples size, we present two representative patients with longitudinal CSF cf-tDNA and

imaging data demonstrating distinct temporal patterns between molecular and imaging biomarkers..

UMich20, a 10-year-old with H3.3K27M DMG was treated pre-progression with dordaviprone after radiation. After an initial increased in ADC at cycle 3, a decline in fraction of tumor with increased ADC in parametric FDM at 220 days indicated an increase in tumor cellularity that was not captured on RAPNO cross-sectional imaging (Figure 4A-B). This coincided with a spike in H3.3K27M plasma tDNA variant allele fraction (VAF) (Figure 4C-D) that we previously demonstrated to be predictive of tumor growth.

UMich 60 was a 19-year-old with thalamic H3.3K27M Tp53 mutant DMG treated pre-progression with dordaviprone post-radiation. She remained on therapy 58.3 months and had best response of 68.8% reduction in cross sectional size prior to progression, consistent with long-term response. Her tumor exhibited persistently elevated fIADC and FDM ratio (Figure 4E), aligned with stable or improving imaging findings (Figure 4F) and concordant reductions in CSF cf-tDNA variant allele frequency across multiple tumor specific mutations (Figure 4G) demonstrating potential for multimodal response assessments.

Metabolic Analysis

Dordaviprone exerts anti-DMG activity by disrupting the TCA cycle, glycolysis, and pyruvate metabolism[15]. To assess whether diffusion imaging correlates with these metabolic effects, we analyzed 7 patients from the pre-progression post radiation dordaviprone cohort with paired ADC imaging and CSF metabolomics at baseline and cycle 3, classifying them by increase or decrease in mean ADC

“Elevated DL-glyceraldehyde 3-phosphate (GA3P) and dihydroxyacetone phosphate (DHAP) were observed in patients with increased ADC, while lactate was enriched in patients with decreased ADC(Figures 5A–C). Following false discovery rate correction, none of these metabolites reached statistical significance.”We then evaluated of reductive stress, measured as the GA3P+DHAP:2-phosphoglyceric acid (2PG) ratio, was higher in the ADC-increased cohort (mean +0.1849) and lower in the ADC-decreased cohort (mean –0.2889) (Figure 5D), consistent with glycolytic disruption from TCA inhibition and NADH accumulation that may block conversion to 1,3-bisphosphoglycerate (1,3-BPG) (Figure 5E).

These findings demonstrate association between diffusion ADC increases to dordaviprone - associated metabolic shifts, suggesting that dynamic diffusion changes may serve as early,

noninvasive markers of treatment response, capturing sub-radiographic tumor evolution prior to conventional imaging detection.

Discussion

This study demonstrates the potential clinical utility of ADC and diffusion-weighted imaging to augment standard-of-care radiographic monitoring in H3K27M DMG. Traditional anatomic assessments, including RAPNO-based cross-sectional and volumetric measures, showed limited predictive value for long-term outcomes at early timepoints, consistent with prior reports in DIPG and DMG.[26] early measurements utilizing two dimension or volumetric assessment did not demonstrate association with outcome, in our study population, volumetric and RAPNO assessments demonstrated high concordance overall, supporting the ongoing utility of cross-sectional measurement as a primary assessment tool.

Diffusion imaging, a widely available modality provided early indications of therapeutic sensitivity and resistance. In the pre-progression, post-radiation cohort treated with dordaviprone, increases in ADC at cycle 3 correlated with both OS and PFS, suggesting that diffusion metrics may capture biologically meaningful treatment effects prior to size-based radiographic change.

Similar to previous studies, baseline to post-radiation did not correlate with overall response. While post-radiation to cycle 3 may represent ADC changes after dordaviprone treatment. the post-radiation timepoint was impacted by early radiation effects which limited the predictive value of post-radiation to cycle 3 timepoint. Baseline to cycle 3 may also represent the culminative effect of radiation and dordaviprone and therefore correlate better with OS and PFS outcomes Baseline ADC characteristics did not predict outcomes in this cohort.[27] In a sub analysis, patients with lower baseline ADC ($<1.10 \times 10^{-3}$ mm²/s) had a median overall survival of 537 days (Supplemental Figure 7), suggesting improved outcomes compared with prior reports. In earlier studies, patients were primarily treated with radiation or other therapies without clear survival benefit. The improved survival observed in this cohort may reflect the addition of dordaviprone, although this finding will require validation in larger cohorts.

Volumetric histogram–based ADC analysis correlated closely with single-slice histogram and radiologist ROI assessments, supporting the feasibility of incorporating such measures into clinical workflows. These findings highlight an opportunity to standardize diffusion imaging as an adjunct biomarker using clinically accessible methods. Nevertheless, ROI placement remains

operator-dependent, and future multicenter studies will be essential to evaluate interobserver variability, reproducibility across platforms, and integration of automated segmentation to enhance precision.[28]

Our primary findings were derived from the pre-progression, post-radiation cohort and were limited by sample size and retrospective design. In addition, the absence of a control cohort of long-term survivors treated without dordaviprone prevents characterization of the natural history of ADC evolution and limits our ability to isolate treatment-specific effects. Larger datasets that include long-term survivors not treated with dordaviprone will be required to more definitively address this question. Decreases in CSF tumor DNA have previously been associated with longer progression-free survival. Differences in sampling time points limited direct comparison with baseline-to–cycle 3 ADC changes in this study. Future studies directly comparing these biomarkers may clarify whether diffusion imaging and CSF tDNA provide complementary measures of early treatment response

Interpretation of imaging metrics in pre-progression patients receiving dordaviprone concurrently was limited by cohort size and a narrow dynamic range of radiographic responses. Prior studies[8, 9, 15] demonstrated limited prognostic value of ADC immediately after radiation therapy. Consistent with these findings, our dataset also demonstrated an early reduction in mean ADC following radiation, which may limit the utility of baseline-to-post-radiation ADC changes as a prognostic biomarker. Similarly, post-progression analyses were constrained by clinical heterogeneity, including prior therapies and variable timing of dordaviprone initiation, complicating interpretation of ADC dynamics in this setting.

Parametric voxel-based assessments using FDM did not show significant associations with survival outcomes. This analysis was limited in statistical power arising from a smaller population studied. fDM necessitated registration across timepoints with baseline to cycle 3 occurring over a median 174 days (range 120-220 days) during which tumor progression, pseudo-progression may impact co-registration across timepoints, area assessed using an intersect VOI and voxel-wise comparisons. Prior applications of fDM involved narrower timeframes concentrating on assessing early radiation induced changes, this analysis instead focused on the period where histogram metrics had demonstrated utility Despite these challenges, integrated anecdotal case analyses combining fDM with serial CSF cf-tDNA data revealed concordant patterns. Early diffusion and molecular changes preceded radiographic progression or durable response, illustrating the potential value of multimodal biomarker integration. Further studies should investigate fDM in a larger cohort, with alternative

comparison timepoints (e.g. post-radiation to subsequent cycles), consider alternative specific thresholds for fiADC/ fdADC and FDM ratio to clarify fDM and its relationship with clinical outcomes.

Mechanistically, dordaviprone is known to disrupt the TCA cycle and glycolytic metabolism.[15] In patients with paired CSF metabolomics, patients with increased ADC demonstrated increased reductive stress reflective dordaviprone -associated metabolic reprogramming. Although ADC is commonly interpreted as reflecting cellular density, dordaviprone may exert multifactorial effects on tumor biology. Treatment with dordaviprone has been shown to induce metabolic disruption and downregulation of cell cycle pathways. Cellular responses to these stressors may influence tumor cellularity, while restoration of H3K27 trimethylation may contribute to microstructural reorganization.[20] Paired radiographic and tissue-based analyses may be required to more fully elucidate the biological mechanisms underlying ADC changes.

Taken together, these data support the integration of diffusion imaging with molecular and metabolic biomarkers to enhance disease monitoring in DMG. Advanced diffusion metrics, when combined with anatomic imaging and liquid biopsy approaches, may enable earlier and more accurate detection of therapeutic response and resistance. Continued validation in prospective, multi-institutional trials will be essential to establish diffusion-based biomarkers as reliable tools for clinical decision-making in this challenging disease. If validated, early diffusion changes such as reduced ADC could help identify patients at risk for poor response before conventional radiographic progression, providing an opportunity to consider therapeutic escalation, enrollment on clinical trials, or rational combination strategies with the goal of improving progression-free and overall survival.

Ethics

Ethical approval for this study was obtained from the University of Michigan IRB. Informed consent was obtained from each patient for collection and analysis of surgical waste samples under the University of Michigan Biorepository and Authorization to Release Protected Health Information (HUM00024610). Samples were acquired from the IRB approved Koschmann Lab Brain Tumor Tissue Repository (REP00000067).

Funding

CK is supported by NIH/NINDS Grant R01-NS124607 and R01-NS119231, NIH/NCI Grant UH2CA302680, Department of Defense Grant CA201129P1, the University of Michigan Chad Carr Pediatric Brain Tumor Center, the ChadTough Defeat DIPG Foundation, Catching Up With Jack, The Pediatric Brain Tumor Foundation, The Yuvaan Tiwari Memorial Foundation, The Morgan Behen Golf Classic, and the Michael Miller Memorial Foundation. BL was supported by the National Institutes of Health under award number T32HL749.

Conflict of Interest

CJG is the co-inventor of PRM licensed to 4DMedical for which he receives royalties. TJS, BF, and MAS are employees of, and hold equity interest in xCures, Inc. TJS, BF and MAS were involved in data curation and did not have direct involvement in analysis or interpretation.

Authorship

Conceptualization: B.C.L., D.P.A., B.A.H., P.S., J.W., T.A., S.J., A.L.G., A.N., Y.C., M.A., S.U., A.F., S.G., S.V., C.L., T.S., C.J.G., H.A.P., M.I., and C.K. Methodology: B.C.L., D.P.A., B.A.H., P.S., C.J.G., Y.C., M.A., and C.K. Data Curation: B.C.L., D.P.A., A.P. J.W., T.A., S.J., A.G., T.J.S., B.F., M.A.S. Formal Analysis: B.C.L., D.P.A., B.A.H., A.P., P.S., C.J.G. H.A.P., M.I.,, and Y.C. Manuscript Preparation (original draft and revisions): B.C L. Supervision: C.K. All authors reviewed and approved the final manuscript.

Data Availability

Deidentified imaging and clinical data will be uploaded to the Children's Brain Tumor Network (CBTN) repository.

Acknowledgements

The authors would like to thank all patients and families for their participation in research. The preparation of this review was not supported by any external funding. The manufacturer of the medication in the publication was offered an opportunity to comment on this article. Changes resulting from comments received were made by the author on the basis of scientific and editorial merit.

References

1. Mackay A, Burford A, Carvalho D, et al. Integrated Molecular Meta-Analysis of 1,000 Pediatric High-Grade and Diffuse Intrinsic Pontine Glioma. *Cancer Cell.* 2017; 32(4):520-537 e525.
2. Hoffman LM, Veldhuijzen van Zanten SEM, Colditz N, et al. Clinical, Radiologic, Pathologic, and Molecular Characteristics of Long-Term Survivors of Diffuse Intrinsic Pontine Glioma (DIPG): A Collaborative Report From the International and European Society for Pediatric Oncology DIPG Registries. *J Clin Oncol.* 2018; 36(19):1963-1972.
3. Miklja Z, Pasternak A, Stallard S, et al. Molecular profiling and targeted therapy in pediatric gliomas: review and consensus recommendations. *Neuro Oncol.* 2019; 21(8):968-980.
4. Cooney TM, Cohen KJ, Guimaraes CV, et al. Response assessment in diffuse intrinsic pontine glioma: recommendations from the Response Assessment in Pediatric Neuro-Oncology (RAPNO) working group. *Lancet Oncol.* 2020; 21(6):e330-e336.
5. Erker C, Tamrazi B, Poussaint TY, et al. Response assessment in paediatric high-grade glioma: recommendations from the Response Assessment in Pediatric Neuro-Oncology (RAPNO) working group. *Lancet Oncol.* 2020; 21(6):e317-e329.
6. Hayward RM, Patronas N, Baker EH, Vezina G, Albert PS, Warren KE. Inter-observer variability in the measurement of diffuse intrinsic pontine gliomas. *J Neurooncol.* 2008; 90(1):57-61.
7. Hargrave D, Chuang N, Bouffet E. Conventional MRI cannot predict survival in childhood diffuse intrinsic pontine glioma. *J Neurooncol.* 2008; 86(3):313-319.
8. Ceschin R, Kocak M, Vajapeyam S, et al. Quantifying radiation therapy response using apparent diffusion coefficient (ADC) parametric mapping of pediatric diffuse intrinsic pontine glioma: a report from the pediatric brain tumor consortium. *J Neurooncol.* 2019; 143(1):79-86.
9. Poussaint TY, Vajapeyam S, Ricci KI, et al. Apparent diffusion coefficient histogram metrics correlate with survival in diffuse intrinsic pontine glioma: a report from the Pediatric Brain Tumor Consortium. *Neuro Oncol.* 2016; 18(5):725-734.
10. Vajapeyam S, Brown D, Billups C, et al. Advanced ADC Histogram, Perfusion, and Permeability Metrics Show an Association with Survival and Pseudoprogression in Newly Diagnosed Diffuse Intrinsic Pontine Glioma: A Report from the Pediatric Brain Tumor Consortium. *AJNR Am J Neuroradiol.* 2020; 41(4):718-724.
11. Arrillaga-Romany I, Gardner SL, Odia Y, et al. ONC201 (Dordaviprone) in Recurrent H3 K27M-Mutant Diffuse Midline Glioma. *J Clin Oncol.* 2024; 42(13):1542-1552.
12. Arrillaga-Romany I, Odia Y, Prabhu VV, et al. Biological activity of weekly ONC201 in adult recurrent glioblastoma patients. *Neuro Oncol.* 2020; 22(1):94-102.
13. Prabhu VV, Madhukar NS, Gilvary C, et al. Dopamine Receptor D5 is a Modulator of Tumor Response to Dopamine Receptor D2 Antagonism. *Clin Cancer Res.* 2019; 25(7):2305-2313.
14. Przystal JM, Cianciolo Cosentino C, Yadavilli S, et al. Imipridones affect tumor bioenergetics and promote cell lineage differentiation in diffuse midline gliomas. *Neuro Oncol.* 2022; 24(9):1438-1451.
15. Venneti S, Kawakibi AR, Ji S, et al. Clinical Efficacy of ONC201 in H3K27M-Mutant Diffuse Midline Gliomas Is Driven by Disruption of Integrated Metabolic and Epigenetic Pathways. *Cancer Discov.* 2023; 13(11):2370-2393.
16. Monje M, Mahdi J, Majzner R, et al. Intravenous and intracranial GD2-CAR T cells for H3K27M(+) diffuse midline gliomas. *Nature.* 2025; 637(8046):708-715.
17. Vitanza NA, Ronsley R, Choe M, et al. Intracerebroventricular B7-H3-targeting CAR T cells for diffuse intrinsic pontine glioma: a phase 1 trial. *Nat Med.* 2025; 31(3):861-868.
18. Cantor E, Wierzbicki K, Tarapore RS, et al. Serial H3K27M cell-free tumor DNA (cf-tDNA) tracking predicts ONC201 treatment response and progression in diffuse midline glioma. *Neuro Oncol.* 2022; 24(8):1366-1374.

19. Yushkevich PA, Piven J, Hazlett HC, et al. User-guided 3D active contour segmentation of anatomical structures: significantly improved efficiency and reliability. *Neuroimage.* 2006; 31(3):1116-1128.
20. Cao Y. Development of image software tools for radiation therapy assessment. *Med Phys.* 2005; 32(6):2136-2136.
21. Klein S, Staring M, Murphy K, Viergever MA, Pluim JP. elastix: a toolbox for intensity-based medical image registration. *IEEE Trans Med Imaging.* 2010; 29(1):196-205.
22. Shamonin DP, Bron EE, Lelieveldt BP, et al. Fast parallel image registration on CPU and GPU for diagnostic classification of Alzheimer's disease. *Front Neuroinform.* 2013; 7:50.
23. Moffat BA, Chenevert TL, Lawrence TS, et al. Functional diffusion map: a noninvasive MRI biomarker for early stratification of clinical brain tumor response. *Proc Natl Acad Sci U S A.* 2005; 102(15):5524-5529.
24. Kerk SA, Lin L, Myers AL, et al. Metabolic requirement for GOT2 in pancreatic cancer depends on environmental context. *Elife.* 2022; 11.
25. Bruzek AK, Ravi K, Muruganand A, et al. Electronic DNA Analysis of CSF Cell-free Tumor DNA to Quantify Multi-gene Molecular Response in Pediatric High-grade Glioma. *Clin Cancer Res.* 2020; 26(23):6266-6276.
26. Lazow MA, Nievelstein MT, Lane A, et al. Volumetric endpoints in diffuse intrinsic pontine glioma: comparison to cross-sectional measures and outcome correlations in the International DIPG/DMG Registry. *Neuro Oncol.* 2022; 24(9):1598-1608.
27. Chen HJ, Panigrahy A, Dhall G, Finlay JL, Nelson MD, Jr., Bluml S. Apparent diffusion and fractional anisotropy of diffuse intrinsic brain stem gliomas. *AJNR Am J Neuroradiol.* 2010; 31(10):1879-1885.
28. Bilgili Y, Unal B. Effect of region of interest on interobserver variance in apparent diffusion coefficient measures. *AJNR Am J Neuroradiol.* 2004; 25(1):108-111.

Figure Legends

Figure 1. Patient selection, baseline characteristics, and molecular features.

(A) Schema demonstrating relation between apparent diffusion coefficient and tumor density with representative images DMG43 with left thalamic DMG with low ADC and DMG35 with pontine DMG with high ADC (B) Overview of patient screening and inclusion for dordaviprone - treated DMG/DIPG cohorts. (C) Tumor location distribution among pre-progression patients. (D) Biopsy and molecular profiling rates. (E) Patient characteristics of the pre-progression population. (F) Oncoplot demonstrating frequency of major mutations

Table 1. Demographic and clinical characteristics of the patients separated by cohort.

Characteristics of patients, age, gender, location, cohort, protocol used.

Figure 2. Conventional size-based imaging metrics do not predict response to dordaviprone.

(A–B) RAPNO assessments of pre-progression patients, (A) spider plot demonstrating change from baseline with representative imaging for long term survivors DMG04 and DMG56, (B)

Waterfall plot of best response, with additional detail provided for long-term survivors excluded from analysis due to unmeasurable disease at cycle 3. Kaplan–Meier curves showing no difference in OS (C–D) or PFS (G-H) by RAPNO cross-sectional or volumetric change. (E&I) Correlation plots confirming no association between size change and survival outcomes.

Figure 3. Early increase in diffusion ADC predicts improved survival in pre-progression, post-radiation patients.

(A) Treatment and imaging timeline. (B) Representative patient cases with T2 Flair and ADC at baseline and cycle 3, representative ADC histogram. (C) Histogram sorted by OS (days) with color correlating with change in ADC increased (red), decreased (blue) (D-E) Kaplan–Meier curves showing longer OS and PFS in patients with increased ADC at cycle 3. (G–H) Positive correlation between ADC change and OS/PFS. (I-J) Kaplan-Meier curves of OS and PFS stratified by tumor location and ADC changes

Figure 4. Multimodal assessment of disease assessment with parametric assessment of ADC and cell free CSF DNA

UMICH-PED 20: (A) Relative tumor size based on RAPNO measurement plotted over time (gray dotted line- right y-axis) compared to fraction of tumor with increased ADC (fIADC) (red line- left y-axis), and fraction of tumor with decreased ADC (fDADC) (blue line- left y-axis). Purple arrow denotes last imaging timepoint prior to progression. (B) Representative MR imaging, T2-FLAIR anatomical imaging, RAPNO based cross-sectional as noted, representative diffusion weighted ADC imaging, scatterplot of fDM assessment, leftmost scatterplot represents legend (C) Plasma H3.3 VAF (orange line, right y-axis) and (D) CSF tDNA VAF plot (blue line (right y-axis) plotted with percent change in RAPNO measurement (gray dotted line-left y-axis) at similar timepoints.

UMED-PED60 (E) Relative tumor size based on RAPNO measurement plotted over time (gray dotted line-right y-axis) compared to fraction of tumor with increased ADC (red line- left y-axis), and fraction of tumor with decreased ADC (blue line- left y-axis). (F) Representative MR imaging, T2-FLAIR anatomical imaging, RAPNO based cross-sectional as noted, (G) CSF tDNA VAF for relevant mutations identified on biopsy including H3F3A purple line, Tp53 R158G (diamonds with light orange lines), Tp53 R248Q (circles with orange line) and PIK3CA (inverted triangles dark orange lint) plotted on the left y-axis plotted with relative RAPNO measurement (gray dotted line-right y-axis) at similar timepoints.

Figure 5. CSF metabolomic correlates link ADC increase to dordaviprone -driven metabolic reprogramming.

(A) Top metabolites with the greatest difference (log2 fold change) between subjects (n=7) with increased ADC compared (pink) compared to decreased ADC (blue) (B) Heatmap of metabolites, patients were stratified across two groups (increasing or decreasing ADC) based on change in ADC from baseline to cycle 3. (C) Volcano plot demonstrating metabolites with significantly different levels from baseline to cycle 3 (D) Reductive stress measured by of the ratio of glyceraldehyde 3- phosphate and dihydroxyacetone phosphate (DHAP) to 2-phosphoglycerate (2PG) was assessed, compared to the subjects with decreasing ADC at cycle 3 patients with increasing ADC exhibited increased reductive stress. (E) Schematic model linking diffusion ADC elevation to metabolic effect. Demonstrating proposed mechanism where dordaviprone inhibits TCA cycle resulting in NADH excess and impedes glycolysis.

Dordaviprone (ONC201)is the first FDA-approved treatment for recurrent H3K27M-mutant diffuse midline glioma, but patient responses vary and no imaging biomarkers currently predict benefit. Diffusion MRI [apparent diffusion coefficient (ADC)], which reflects tumor cellularity, is obtained during routine care. In patients treated with dordaviprone after radiation and before progression, early changes in tumor size did not predict survival. However, tumors showing increased ADC after two cycles were associated with longer overall survival and delayed progression. Anecdotal analyses of spinal fluid metabolites showed patterns consistent with dordaviprone's expected biological effects, supporting further study of early ADC increase as a potential biomarker.

Table 1: Demographic and clinical characteristics of the patients separated by cohort.

	Pre-Progression Concurrent Radiation and Dordaviprone (n=6)		Pre-progression Post-Radiation Dordavirpone (n=21)		Post-Progression Patients (n=11)	
Sex (n,%)						
Male	4	66.6%	16	76.2%	6	54.5%
Female	2	33.30%	5	23.8%	5	45.5%
Age at Diagnosis (years)						
Mean	9.58	Range (5-15)	13	Range (3-44)	21.04	Range (2-54)
Age>18	0	0%	2	9.5%	5	45.45%
Location (n,%)						
Brainstem	4	66.6%	14	66.7%	4	36.4%
Thalamic	2	33.3%	6	28.6%	4	36.4%
Other	0	0	1	4.8%	3	27.3%
Histopathological Diagnosis						
Yes	5	83.3%	18	85.7%	10	90.9%
No	1	16.7%	3	14.3%	1	9.1%
Protocol (n.%)						
EAP	0	0	12	57.1%	10	90.9%
ONC014	6	100	9	42.8%	1	9.1%

*EAP denotes expanded access protocol

Figure 1

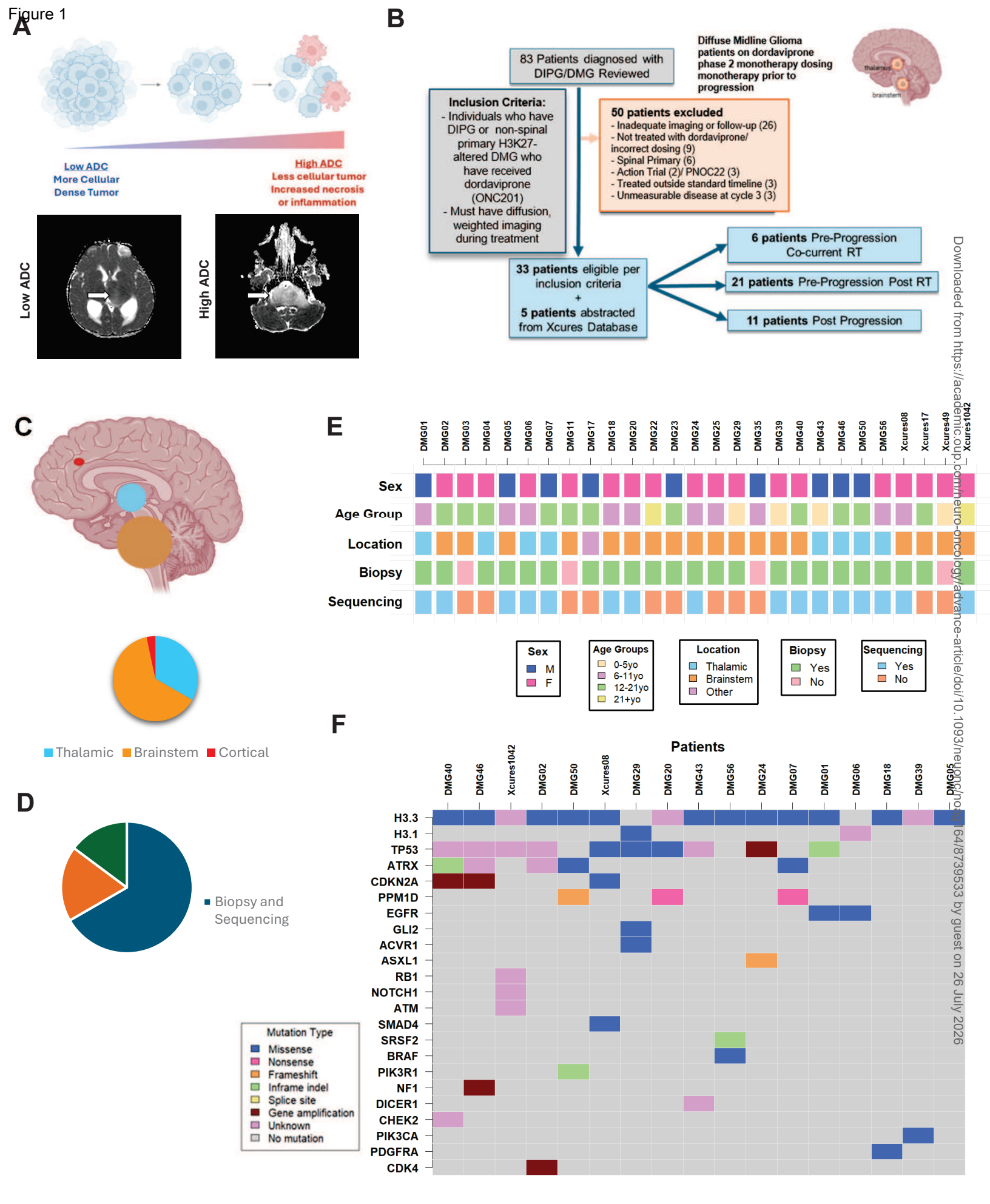

Figure 2

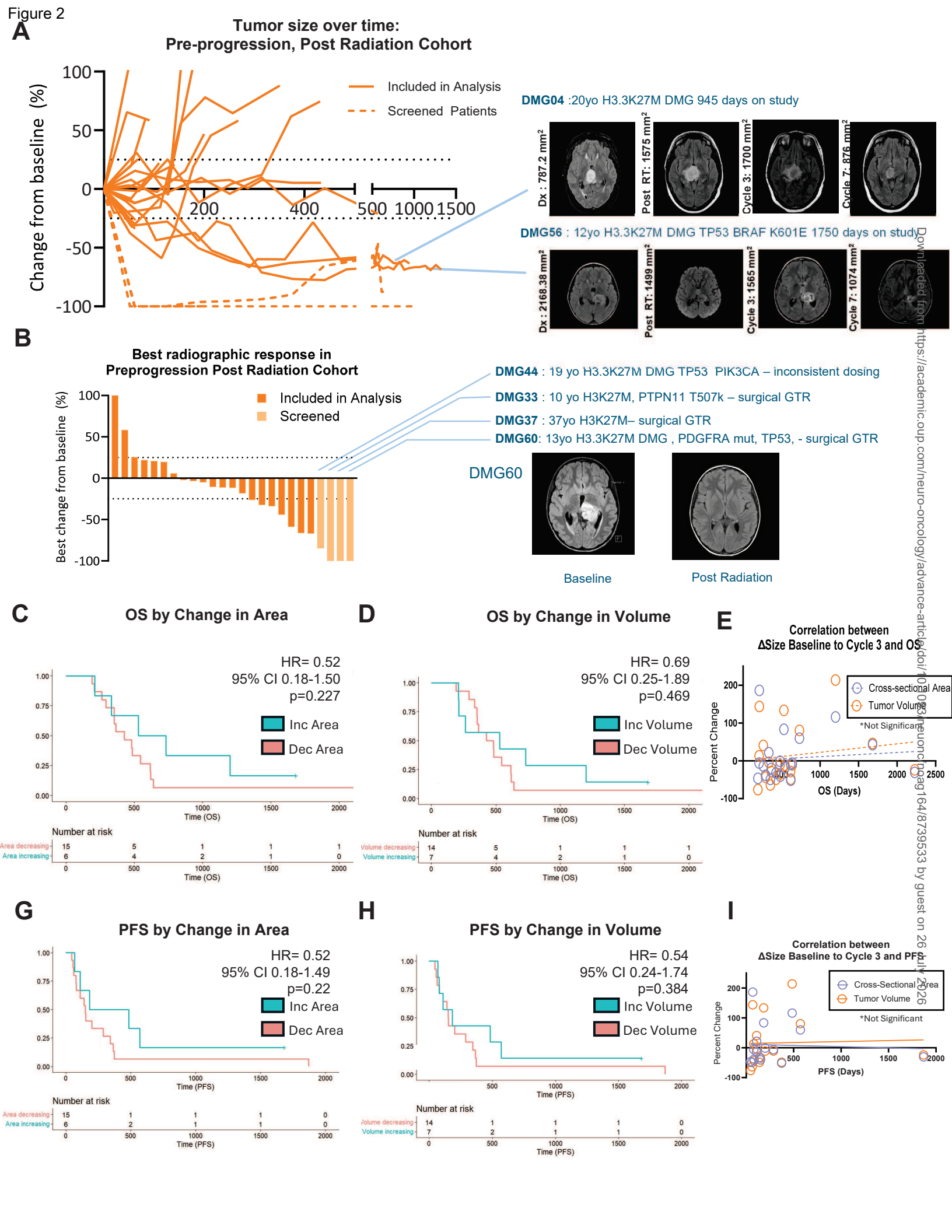

Figure 3

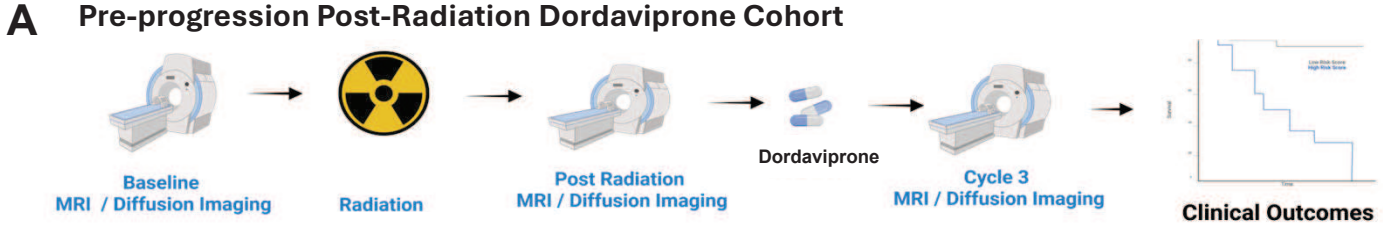

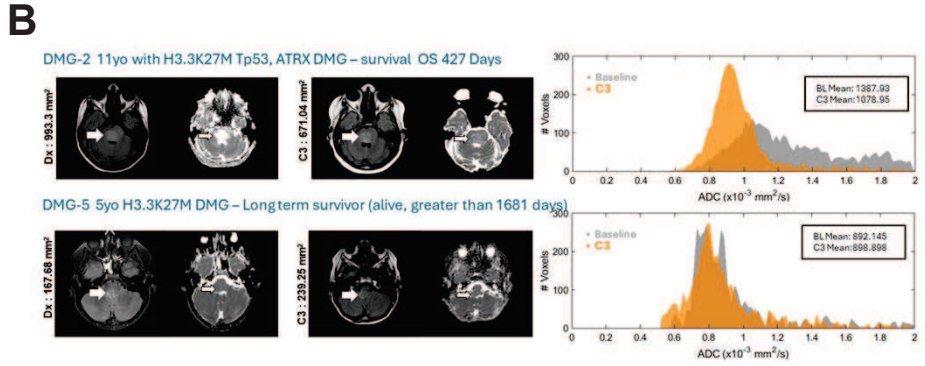

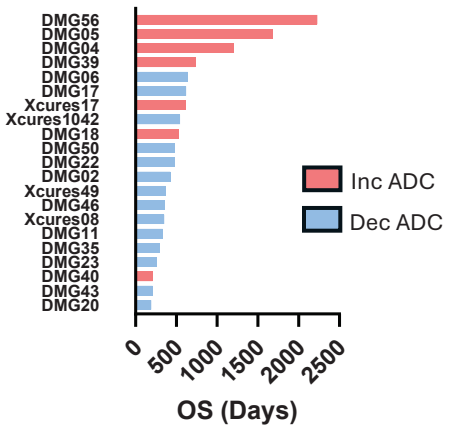

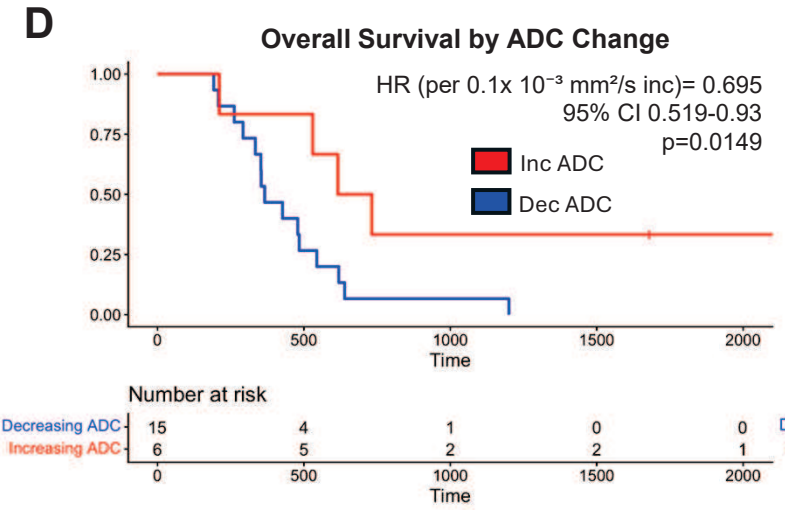

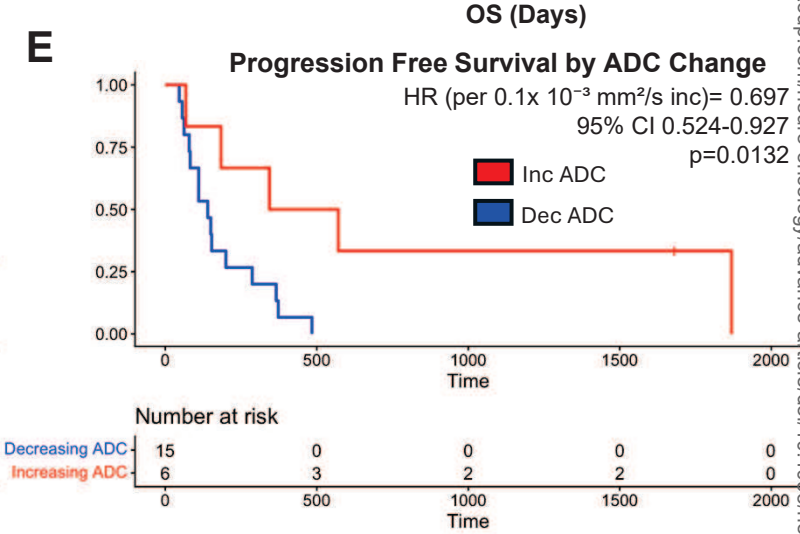

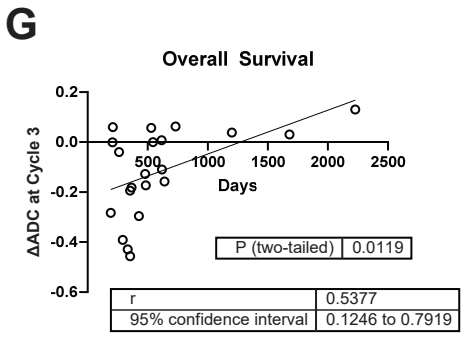

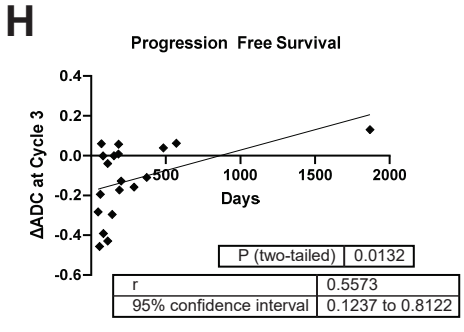

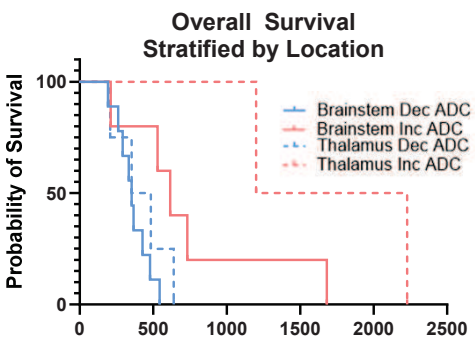

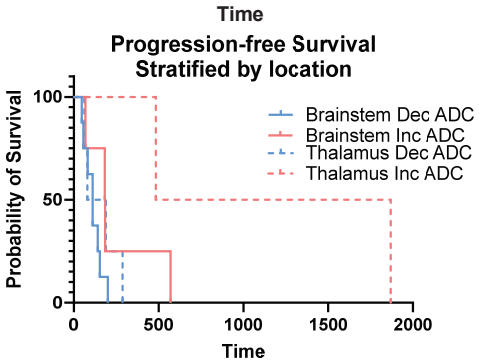

Figure 4

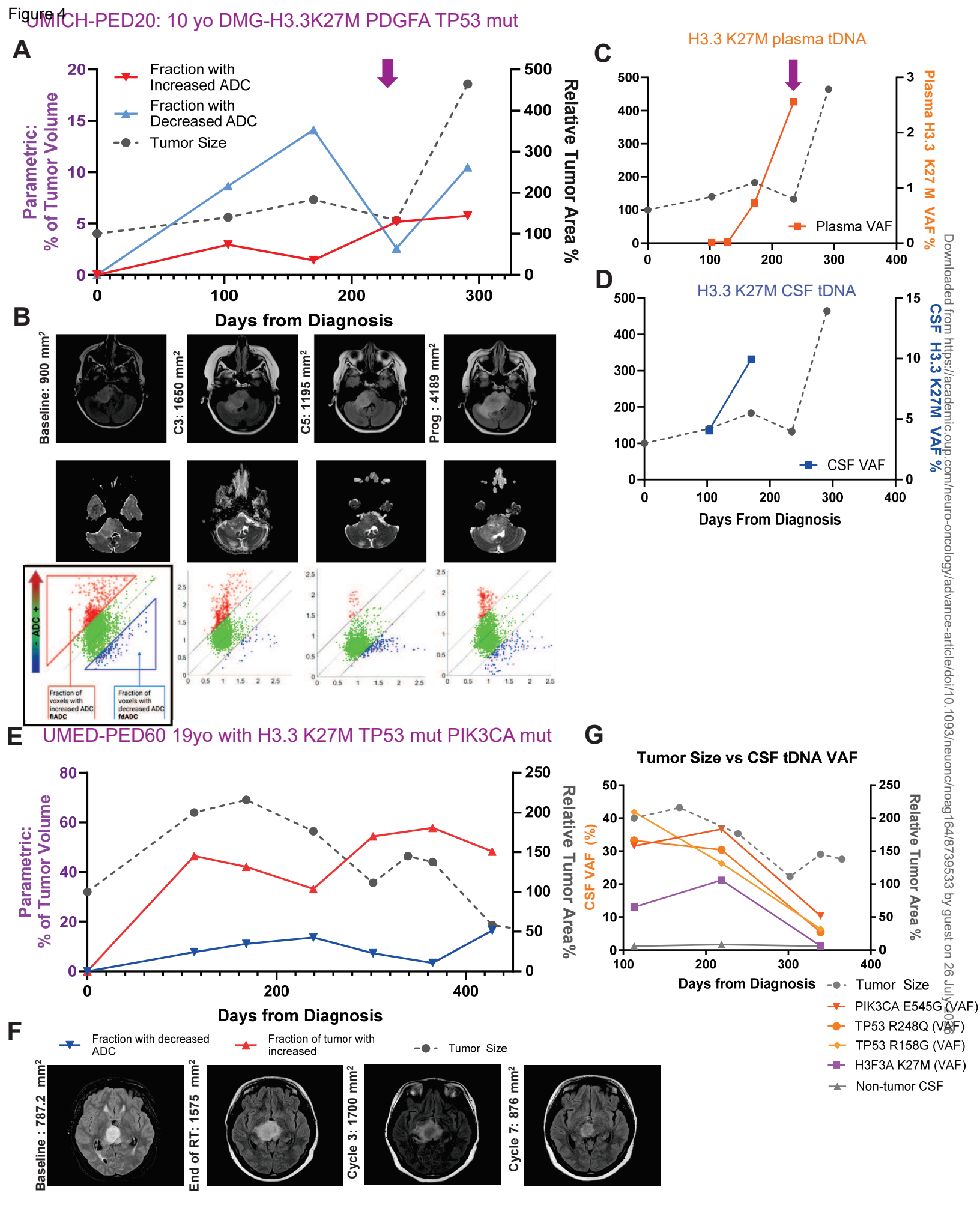

Figure 5

CSF metabolomic delta vs ADC delta